



# Engineering of charge transport materials for universal low optimum doping concentration in phosphorescent organic light-emitting diodes

Chang Woo Seo<sup>a</sup>, Ji Hwan Yoon<sup>b</sup>, Jun Yeob Lee<sup>a,\*</sup>

<sup>a</sup> Department of Polymer Science and Engineering, Dankook University, 126, Jukjeon-dong, Suji-gu, Yongin-si, Gyeonggi-do 448-701, Republic of Korea

<sup>b</sup> Samsung Mobile Display, San #24, Nongseo-dong, Giheung-gu, Yongin-si, Gyeonggi-do 446-711, Republic of Korea

## ARTICLE INFO

### Article history:

Received 26 July 2011

Received in revised form 15 November 2011

Accepted 17 November 2011

Available online 2 December 2011

### Keywords:

Phosphorescent organic light emitting diodes

Low doping concentration

High efficiency

Charge trapping

## ABSTRACT

A universal low optimum doping concentration of below 5% was demonstrated in phosphorescent organic light-emitting diodes (PHOLEDs) by managing the energy levels of charge transport materials. The device performances of PHOLEDs could be optimized at a low doping concentration of 3% irrespective of the host material in the emitting layer. The suppression of charge trapping and hopping by the dopant through charge transport layer engineering optimized the device performance at low doping concentration. In addition, it was revealed that PHOLEDs with low optimum doping concentration show better quantum efficiency, low efficiency roll-off and low doping concentration dependency of the device performance.

© 2011 Elsevier B.V. All rights reserved.

## 1. Introduction

Phosphorescent organic light-emitting diodes (PHOLEDs) have been developed to improve the quantum efficiency of common fluorescent organic light-emitting diodes (FOLEDs) [1]. There have been many papers reporting over 20% external quantum efficiency in PHOLEDs compared with 5–10% external quantum efficiency in FOLEDs [2–5]. Both singlet and triplet exciton harvesting enhanced the quantum efficiency of PHOLEDs.

In general, the quantum efficiency of PHOLEDs was optimized at a doping concentration of 5–20% [1–9], although there have been a few works reporting low optimum doping concentrations of below 5% [5,10,11]. Typically, the optimum doping concentration of PHOLEDs was much higher than the optimum doping concentration of 0.5–5% of FOLEDs. The quantum efficiency of FOLEDs was degraded at high doping concentration due to a strong concentration quenching effect, leading to low optimum doping concentration in FOLEDs [12,13]. However, it was reported that

the concentration quenching effect was not as significant in PHOLEDs as it was in FOLEDs, resulting in high optimum doping concentration in PHOLEDs. However, a few works reported optimum doping concentration of below 5% in PHOLEDs [5,10,11]. Efficient energy transfer from specific host to dopant was proposed as the origin for the low optimum doping concentration of PHOLEDs. It was reported that low optimum doping concentration could be obtained in some specific host materials with effective energy transfer from host to dopant [10]. However, it is not clear how the device performances can be optimized at either low or high doping concentration. Therefore, a systematic study to elucidate the origin of the optimum doping concentration of PHOLEDs is strongly required. In addition, the development of a PHOLED with low optimum doping concentration is necessary to reduce the production cost of OLED panels through a reduction in the amount of dopant used.

In this work, the origin of the optimum doping concentration of PHOLEDs was systematically studied using various host and charge transport materials. It was demonstrated that triplet host materials can be made to show low optimum doping concentrations of below 5% by managing

\* Corresponding author. Tel./fax: +82 31 8005 3585.

E-mail address: [leej17@dankook.ac.kr](mailto:leej17@dankook.ac.kr) (J.Y. Lee).

the energy levels of the hole and electron transport materials. Suppression of charge trapping by the dopant enabled the fabrication of PHOLEDs with optimum doping concentration below 5%. This work discovered and proved that the optimum doping concentration of PHOLEDs is below 5%. In addition, it was revealed that the device performances of PHOLEDs can be improved by optimizing device performances at low doping concentration.

## 2. Experimental

Several host materials, bis-9,9'-spiro[fluoren-2-yl]-methanone (BSFM), 1,3-di(9*H*-carbazol-9-yl)benzene (mCP), 9-(3-(9*H*-carbazole-9-yl)phenyl)-3-(dibromophenylphosphoryl)-9*H*-carbazole (mCPPO1), 4,4',4''-trismm?>(N-carbazolyl)triphenylamine (TCTA) and 1,3,5-tris(N-phenylbenzimidazole-2-yl)benzene (TPBI), were used as host materials for the emitting layer to investigate the effect of the host material properties on the optimum doping concentration of PHOLEDs. BSFM, TCTA and TPBI were doped with green-emitting (III) tris(2-phenylpyridine) (Ir(ppy)<sub>3</sub>), while mCP and mCPPO1 were doped with blue-emitting iridium(III) bis-(4,6-difluorophenylpyridinato) picolinate (Flrpic). The hole transport materials were 4,4'-(cyclohexane-1,1-diyl)bis(N-phenyl-N-p-tolylaniline) (TAPC), TCTA, 4,4'-di(9*H*-carbazol-9-yl)biphenyl (CBP) and mCP, depending on the emitting layer, and the electron transport materials were diphenylphosphine oxide-4-(triphenylsilyl)phenyl (TSPO1), 2-diphenylphosphine oxide-9,9'-spirobifluorene (SPPO1), 2,7-bis(diphenylphosphoryl)-9,9'-spiro[fluorene] (SPPO13) and BSFM. All charge transport materials used in this work possessed higher triplet energies than the emitting materials to suppress triplet exciton quenching by the charge transport layers. Hole transport materials with different highest occupied molecular orbital (HOMO) levels were chosen to study the relationship between the HOMO level of the hole transport material and the optimum doping concentration, while electron transport materials with different lowest unoccupied molecular orbital (LUMO) levels were selected in order to correlate the LUMO level of the electron transport material with the optimum doping concentration. The chemical structures of the host, hole transport and electron transport materials are summarized in Table 1. The HOMO, LUMO and triplet energies of the host materials are also included in the table.

A basic device structure of indium tin oxide (ITO, 150 nm)/N,N'-diphenyl-N,N'-bis-[4-(phenyl-*m*-tolyl-amino)-phenyl]-biphenyl-4,4'-diamine (DNTPD, 60 nm)/N,N'-di(1-naphthyl)-N,N'-diphenylbenzidine (NPB, 25 nm)/hole transport material (5 nm)/host:dopant (30 nm, 3% or 5% or 10%)/electron transport layer (5 nm)/TSPO1 (20 nm)/LiF(1 nm)/Al(200 nm) was used for the device fabrication. The doping concentrations were 3%, 5% and 10%. All devices were fabricated by vacuum thermal evaporation and encapsulated with a glass lid after device fabrication. Device performances of the PHOLEDs were measured by using a Keithley 2400 source measurement unit and a CS 1000 spectroradiometer. Solid photoluminescence (PL) spectra of the doped film were

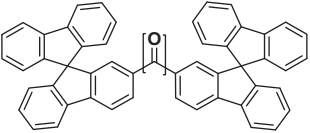
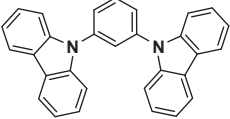
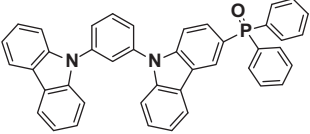
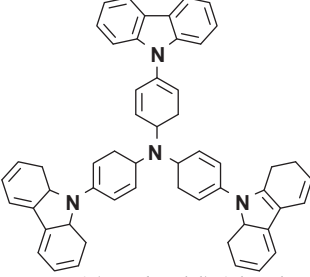
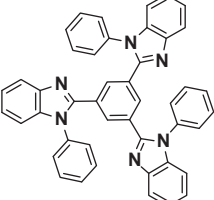
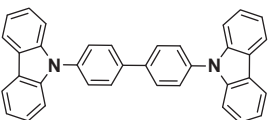
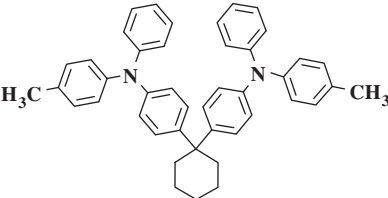
analyzed using a fluorescence spectrometer. The thickness of the doped solid film was 30 nm and the PL intensity of the doped film was measured.

## 3. Results and discussion

The quantum efficiency of PHOLEDs generally depends on the charge balance in the emitting layer, which is largely determined by the densities of holes and electrons in the emitting layer. The densities of holes and electrons are greatly dependent on the energy levels of the host and dopant materials. If there is a large difference between the energy levels of the host and dopant materials, charge trapping and hopping by the dopant are the main mechanism of charge transport [14–16] and charge trapping is the dominant process for light emission. On the contrary, if there is little difference between the energy levels, charge transport through the host material is dominant and energy transfer from host to dopant is the main mechanism for light emission. Once the host and dopant materials are fixed, the charge trapping and hopping are affected by the energy levels of the charge transport materials. A large energy level difference between the host and charge transport materials induces more charge trapping, leading to light emission by charge trapping mechanism rather than energy transfer. On the other hand, smaller energy level difference induces less charge trapping by the dopant and more energy transfer from host to dopant. Therefore, the charge balance and light emission process in the emitting layer can be managed by the charge transport material, indicating that the optimum doping concentration may be affected by the energy level difference between the host and charge transport materials. Based on this concept, the energy levels of charge transport materials were controlled in order to study their influence on the optimum doping concentration of PHOLEDs. Depending on the charge transport properties of the host materials, either the hole transport layer or the electron transport layer was managed. The basic device structure of the PHOLEDs is shown in Fig. 1. The thickness of the hole transport and electron transport materials was 5 nm to minimize the effect of charge transport mobility on the device performances.

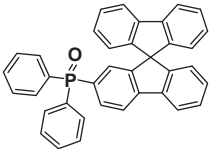
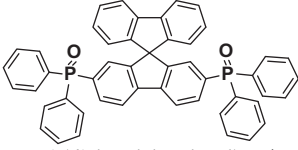
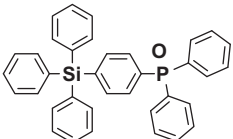
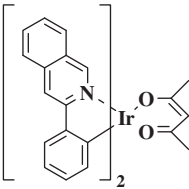
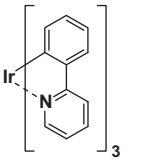
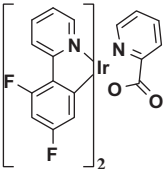
As a hole trapping device with a large HOMO level difference between the host and dopant materials, the BSFM:Ir(ppy)<sub>3</sub> device was fabricated. BSFM is an electron transport type host which shows a large HOMO level difference with the Ir(ppy)<sub>3</sub> dopant. The energy level diagram of the device is shown in Fig. 2. Three green PHOLEDs with different hole transport materials were fabricated. Three hole transport materials, TAPC, TCTA and CBP, were used and the emitting layer was BSFM:Ir(ppy)<sub>3</sub>. The electron transport material was also BSFM. The triplet energy of the TAPC (2.9 eV), TCTA (2.7 eV) and CBP (2.6 eV) was higher than that of the Ir(ppy)<sub>3</sub> (2.4 eV) and therefore a triplet exciton quenching effect by the hole transport layer could be excluded [17,18]. In addition, the thickness of the hole transport layer (5 nm) was minimized to maintain the current density of the device at a similar value irrespective of the hole transport material used. Fig. 3 shows the current

**Table 1**  
Chemical structures and energy levels of organic materials.

Name	Chemical structure	HOMO (eV)	LUMO (eV)	Triplet energy (eV)
BSFM	 9,9'-Spirobi[fluorene]-2-yl(9,9'-spirobi[fluorene]-7-yl)methanone	5.9	2.8	2.60
mCP	 1,3-Di(9H-carbazol-9-yl)benzene	6.1	2.4	2.9
mCPPO1	 9-(3-(9H-Carbazol-9-yl)phenyl)-3-(diphenylphosphoryl)-9H-carbazole	6.13	2.64	3.0
TCTA	 4,4',4''-Tris(N-carbazolyl)triphenylamine	5.7	2.4	2.8
TPBI	 1,3,5-Tris(1-phenyl-1H-benzo[d]imidazol-2-yl)benzene	6.1	2.8	2.6
CBP	 4,4'-Di(9H-carbazol-9-yl)biphenyl	5.9	2.6	2.6
TAPC	 4,4'-(Cyclohexane-1,1-diyl)bis(N-phenyl-N-p-tolylaniline)	5.50	2.00	2.87
SPP01		6.56	2.74	2.79

(continued on next page)

Table 1 (continued)

Name	Chemical structure	HOMO (eV)	LUMO (eV)	Triplet energy (eV)
SPPO13	 2-Diphenylphosphine oxide-9,9'-spirobifluorene	6.52	2.87	2.73
TSPO1	 2,7-Bis(diphenylphosphoryl)-9,9'-spirobi[fluorene]	6.79	2.52	3.19
Ir(pq) <sub>2</sub> acac	 Diphenylphosphine oxide-4-(triphenylsilyl)phenyl	5.2	3.0	2.2
Ir(ppy) <sub>3</sub>	 Iridium(III) bis-(2-phenylquinoline) acetylacetonate	5.2	2.8	2.4
Firpic	 fac-Tris(2-phenylpyridine)iridium	5.70	3.05	2.65
	 Iridium(III) bis(4,6-(difluorophenyl)-pyridinato-N,C') picolinate			

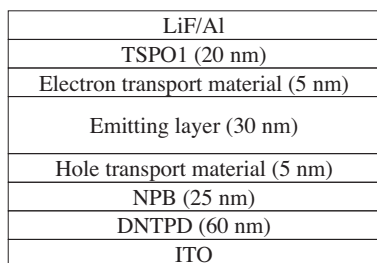
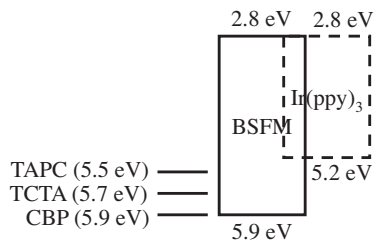


Fig. 1. Basic device structure PHOLEDs used in this work.

Fig. 2. Energy level diagram of BSFM:Ir(ppy)<sub>3</sub> devices with different hole transport materials.

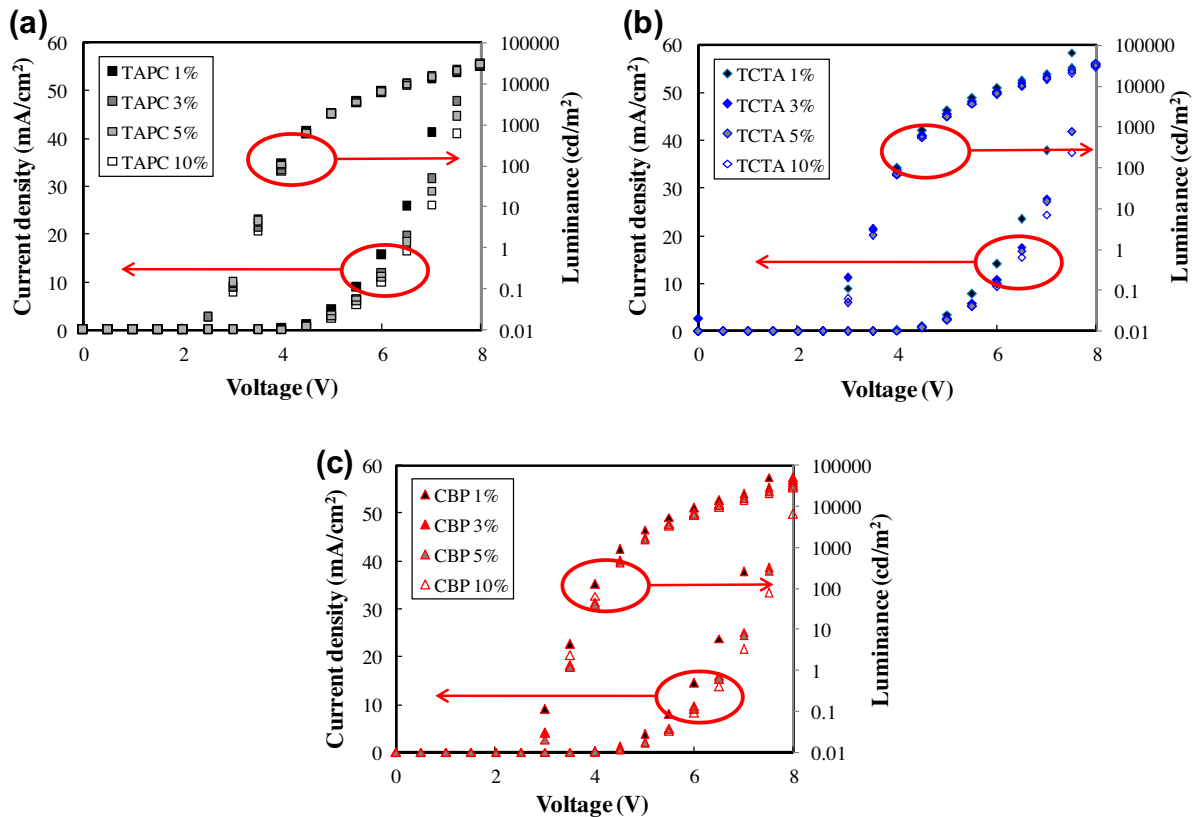


Fig. 3. Current density–voltage–luminance curves of BSFM:Ir(ppy)<sub>3</sub> devices with TAPC (a), TCTA (b) and CBP (c) hole transport layers.

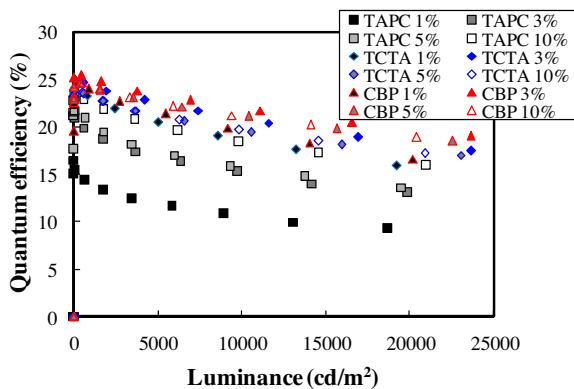


Fig. 4. Quantum efficiency–luminance curves of BSFM:Ir(ppy)<sub>3</sub> devices with TAPC, TCTA and CBP hole transport layers.

density–voltage–luminance curves of green PHOLEDs with different hole transport materials according to the doping concentration of Ir(ppy)<sub>3</sub>. The current densities of the three devices were similar, although they slightly decreased in response to an increase of doping concentration due to the charge trapping effect by the dopant, as reported in other works [16]. The change in the current density according to the doping concentration was significant in the TAPC device compared to in the TCTA and CBP devices. As can be seen in the energy level diagram, the probability

of direct charge injection from the hole transport layer to the dopant is high in the TAPC device, leading to a relatively large dependence of the current density on the doping concentration.

Quantum efficiency–luminance curves of the green PHOLEDs are shown in Fig. 4 according to the doping concentration of Ir(ppy)<sub>3</sub>. The relationship between the doping concentration and the quantum efficiency was quite different depending on the hole transport material. The quantum efficiencies of the TCTA and CBP devices were optimized at a doping concentration of 3%, while that of the TAPC device was optimized at a doping concentration of 10%. In addition, the quantum efficiency of the TAPC device was lower than those of the TCTA and CBP devices, and was greatly dependent on the doping concentration. The difference between the dependences of the quantum efficiency on the doping concentration can be explained by the hole trapping effect of the dopant in the emitting layer. As explained earlier, the charge trapping by dopant is the dominant mechanism for the charge transport and light emission when the energy barrier between the hole transport layer and host material is large. In the case of TAPC, there is a large energy barrier of 0.4 eV for hole injection between TAPC and the BSFM host material, which hinders the hole injection from TAPC to the BSFM host material and induces hole injection directly into the dopant material. As holes are injected and transported through the dopant materials by hole hopping, the hole density depends on

the doping concentration. Therefore, doping concentration is critical to the charge balance, resulting in an optimum doping concentration of 10%.

In contrast, the optimum doping concentration of the TCTA and CBP devices was 3%. The energy barriers for hole injection of the TCTA and CBP devices were 0.2 eV and 0 eV, respectively, which were lower than that of the TAPC device (0.4 eV). The reduced energy barriers of the TCTA and CBP devices change the hole injection mechanism, so that hole injection from the hole transport layer to the host is the dominant hole injection mechanism. As less holes are trapped and transported by the dopant in the TCTA and CBP devices, the doping concentration does not greatly affect the charge balance in the emitting layer. In addition, the light emission is dominated by the energy transfer from host to dopant materials. Therefore, the quantum efficiency of the green PHOLEDs was optimized at 3%, which corresponds to the optimum doping concentration for solid PL emission. In addition, the quantum efficiency was not greatly affected by the doping concentration. The quantum efficiency followed the same tendency as the PL intensity, which will be shown in Fig. 5.

Fig. 5 shows the PL emission intensity of the solid film of BSMF:Ir(ppy)<sub>3</sub> according to the doping concentration of Ir(ppy)<sub>3</sub>. The BSMF host was excited by UV light. The PL intensity of the solid film was decreased according to the increase of doping concentration, due to a concentration quenching effect between dopant materials. As the PL emission is due to the energy transfer from host to dopant material without any charge trapping effect, the optimum doping of PL emission is that of energy transfer process. Considering that the optimum doping concentration for the PL intensity was the same as the optimum doping concentration of TCTA and CBP devices, the dominant light emission mechanism of light emission in TCTA and CBP devices is energy transfer. However, the optimum doping concentration of TAPC device was different from that of PL emission, proving that charge trapping is the dominant light emission mechanism. Therefore, it can be concluded that the device performances are optimized at low doping concentration when energy transfer is the main process for light emission, while they are optimized at high doping concentration when charge trapping is the dominant process for light emission. In addition, the effect of the doping concentration on the quantum efficiency was not significant in the TCTA and CBP devices, for which

similar quantum efficiencies were observed. However, the quantum efficiency of the TAPC device was greatly dependent on the doping concentration due to charge trapping by the dopant materials.

The maximum quantum efficiency of the CBP device was 25.4% and the quantum efficiency at 1000 cd/m<sup>2</sup> was 25.1% at 3% doping concentration. The maximum quantum efficiency and the quantum efficiency at 1000 cd/m<sup>2</sup> of the TCTA device were 24.9% and 24.5%, respectively. Although the quantum efficiency of the TCTA device was slightly lower than that of the CBP device, both devices showed high quantum efficiency and little efficiency roll-off. However, the maximum quantum efficiency and the quantum efficiency at 1000 cd/m<sup>2</sup> of the TAPC device were 23.1% and 22.5%, which were lower than those of the TCTA and CBP devices. As the quantum efficiency was optimized at 10% doping concentration, which shows a rather weak PL intensity (Fig. 5), the absolute value of the quantum efficiency was degraded in the TAPC device. Therefore, it is better to fabricate devices with optimum doping concentration below 5% to achieve high quantum efficiency.

Based on the hole trapping result for the optimization of device performances at doping concentrations below 5%, electron trapping devices based on the hole transport type mCP host were also fabricated. There have been many papers reporting high quantum efficiency for devices using common mCP as the host material [6,19–21]. In all device data, the optimum doping concentration was in the range from 5% to 20% and no paper reporting below 5% optimum doping concentration has been published. The problem in other works which prevented low optimum doping concentration was the high energy barrier for electron injection from the electron transport layer to the host. The LUMO level of the mCP is 2.4 eV and it was difficult to reduce the energy barrier for electron injection using common electron transport materials. Therefore, the dominant electron injection mechanism for the mCP device was direct electron injection from the electron transport layer to the dopant, which meant that the device performance was optimized at a high doping concentration of more than 5%. However, the device performances of mCP devices can be optimized at a doping concentration below 5% simply by managing the electron transport layer.

The PL intensity of the solid film of mCP:Flrpic was monitored according to the doping concentration to confirm the optimum doping concentration for light emission

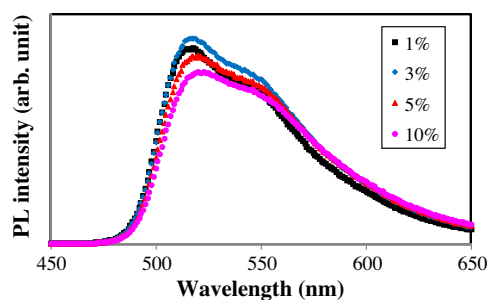


Fig. 5. Photoluminescence spectra of BSMF:Ir(ppy)<sub>3</sub> solid film according to doping concentration. The solid film was excited at 339 nm.

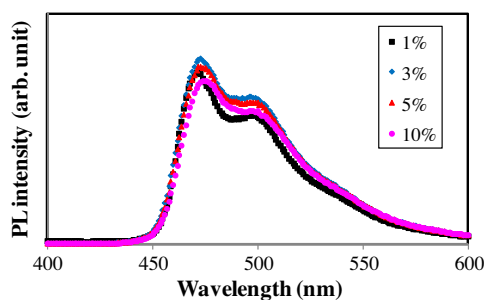


Fig. 6. Photoluminescence spectra of mCP:Flrpic solid film according to doping concentration. The solid film was excited at 339 nm.

through energy transfer process before fabricating mCP based blue PHOLEDs. Fig. 6 shows the PL intensity of solid films of mCP:Flrpic according to doping concentration. The PL intensity was maximized at 3% doping concentration and reduced at high doping concentration. Therefore, the optimum doping concentration for light emission by energy transfer process is 3% in the mCP:Flrpic emitting layer.

Three devices with different electron transport layers were fabricated. TSPO1, SPPO1 and SPPO13 were used as the electron transport materials for mCP:Flrpic devices. All three materials have a triplet energy over 2.70 eV and so the exciton quenching effect on the quantum efficiency by the electron transport layer can be excluded. The LUMO levels of the electron transport layer were 2.52 eV (TSPO1), 2.70 eV (SPPO1) and 2.84 eV (SPPO13), enabling the study of the effect of LUMO levels on the optimum doping concentration of mCP:Flrpic devices. The energy barriers for electron injection from the electron transport layer to the emitting layer were 0.12 eV (TSPO1), 0.30 eV (SPPO1) and 0.44 eV (SPPO13). The energy level diagram of the mCP:Flrpic devices is shown in Fig. 7. The thickness of the electron transport layer was 5 nm and a 20 nm TSPO1 layer was deposited on the electron transport layer. The thickness of each electron transport layer was minimized to keep the current density of the devices constant.

Fig. 8 shows the quantum efficiency–luminance curves of the mCP:Flrpic devices with different electron transport

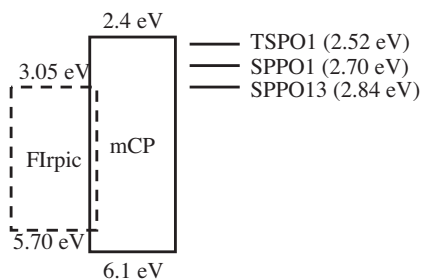


Fig. 7. Energy level diagram of mCP:Flrpic devices with different electron transport materials.

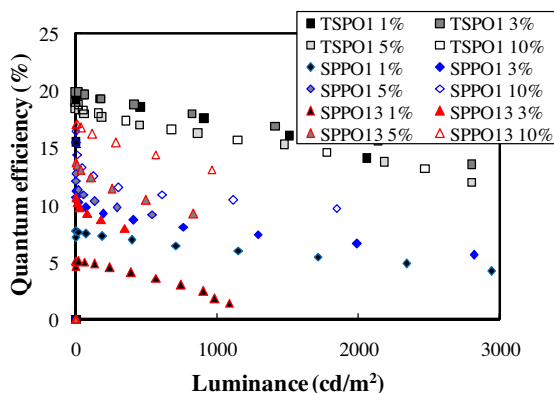


Fig. 8. Quantum efficiency–luminance curves of mCP:Flrpic device with different electron transport materials.

layers. The quantum efficiency of the mCP:Flrpic device with the TSPO1 electron transport layer was optimized at 3% doping concentration and was reduced at high doping concentration, while the quantum efficiency of the mCP:Flrpic devices with SPPO1 and SPPO13 electron transport layers was optimized at 10%. The maximum quantum efficiencies of the mCP:Flrpic devices were 19.8%, 16.4% and 17.1% for TSPO1, SPPO1 and SPPO13, respectively. The quantum efficiency of the TSPO1 device, which was optimized at 3%, was higher than those of the SPPO1 and SPPO13 devices with an optimum doping concentration of 10%. Similarly to the BSFM device, the device with low optimum doping concentration showed better quantum efficiency than that with high optimum doping concentration. In addition, the doping concentration had little effect on the quantum efficiency in the mCP:Flrpic device with low optimum doping concentration, while it was critical to the quantum efficiency in the mCP:Flrpic device with high optimum doping concentration. As electron trapping by the dopant are the main mechanisms for electron injection and light emission in the SPPO1 and SPPO13 devices, due to the large energy barrier for electron injection, the doping concentration had a large effect on the charge balance in the emitting layer, leading to strong dependence of the quantum efficiency on the doping concentration. In the case of TSPO1, there was a difference of only 0.12 eV between the energy levels of the mCP host and TSPO1, which led to little doping concentration dependence of the quantum efficiency as the electron injection and transport are dominated by the host and light emission is caused by energy transfer from host to dopant. This result agreed with the data obtained in the BSFM device, proving that management of the energy levels of charge transport layers enables the optimization of device performance at a low doping concentration of below 5%. This is the first work reporting a low optimum doping concentration of 3% in mCP:Flrpic devices.

The concept of managing the light emission mechanism through engineering energy levels of charge transport materials to optimize the device performance at low doping concentration was confirmed in other host materials. A bipolar type host material, mCPP01, was doped with Flr-

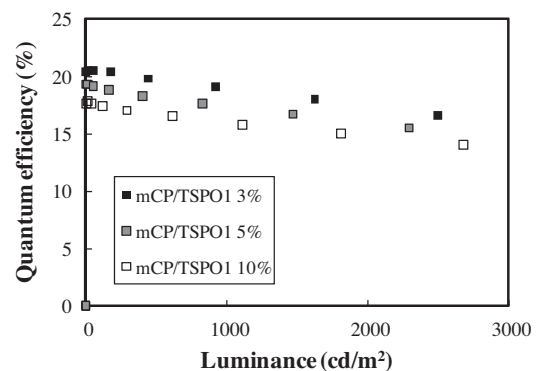


Fig. 9. Quantum efficiency–luminance curves of the mCPP01:Flrpic devices according to doping concentration. Device structure was ITO/DNTPD/NPB/mCP/mCPP01:Flrpic/TSPO1/LiF/Al.



pic and sky blue PHOLEDs were fabricated. The hole transport material was mCP and the electron transport material was TSPO1. The energy barrier for hole injection was 0.03 eV and that for electron injection was 0 eV. The doping concentrations of the mCPPO1 device were 3%, 5% and 10%. Quantum efficiency–luminance curves of the mCPPO1:Flrpic devices are shown in Fig. 9. The quantum efficiency was optimized at 3% and a high quantum efficiency of over 20% was obtained in the mCPPO1:Flrpic device. The quantum efficiency was decreased according to the doping concentration, but the efficiency was reduced by only 15% even at 10% doping concentration. The efficiency roll-off was also not significant in the mCPPO1:Flrpic device. As there was little energy barrier for charge injection, the energy transfer was the main mechanism for light emission and the device performance was optimized at a doping concentration of 3% for maximum PL emission.

A strong hole transport type host material, TCTA, was also evaluated to prove that the device performances of triplet host materials can be optimized at low doping concentration. Green-emitting Ir(ppy)<sub>3</sub> was doped as the green phosphorescent material. The hole transport material was TCTA and the electron transport material was TSPO1. The energy barrier for hole injection was 0 eV and that for electron injection was 0.12 eV. Both hole and electron energy barriers were minimized by controlling the energy levels of the hole and electron transport layers. Quantum efficiency–luminance curves of the TCTA:Ir(ppy)<sub>3</sub> PHOLEDs are shown in Fig. 10. The quantum efficiency was optimized at a doping concentration of 3% and was reduced according to the increase of the doping concentration. Although the maximum quantum efficiency of the TCTA:Ir(ppy)<sub>3</sub> device was only 14.3% due to the strong hole transport and poor electron transport properties of the TCTA, the optimum doping concentration was 3%. Similarly to other devices that were optimized at low doping concentration, the efficiency roll-off and the reduction of the quantum efficiency at high doping concentration were not significant even at 10% doping concentration.

A common electron transport type host, TPBI, was also tested as a green host material. The doping concentrations

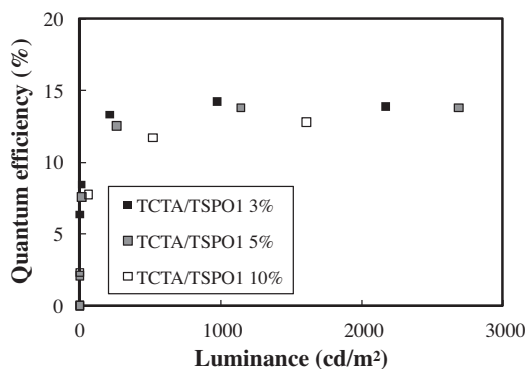


Fig. 10. Quantum efficiency–luminance curves of the TCTA:Ir(ppy)<sub>3</sub> devices according to doping concentration. Device structure was ITO/DNTPD/NPB/TCTA/TCTA:Ir(ppy)<sub>3</sub>/TSPO1/LiF/Al.

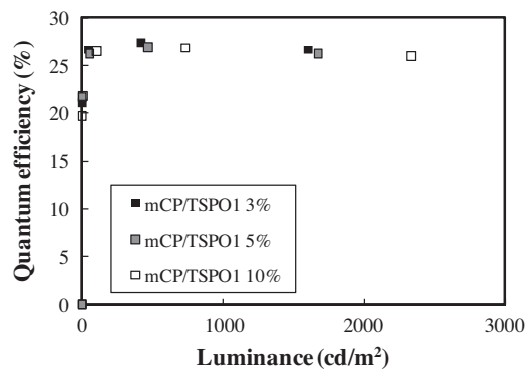


Fig. 11. Quantum efficiency–luminance curves of the TPBI:Ir(ppy)<sub>3</sub> devices according to doping concentration. Device structure was ITO/DNTPD/NPB/mCP/TPBI:Ir(ppy)<sub>3</sub>/TSPO1/LiF/Al.

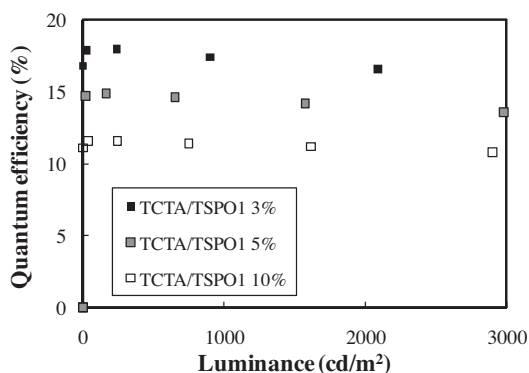


Fig. 12. Quantum efficiency–luminance curves of the BSFM:Ir(pq)<sub>2</sub>acac devices according to doping concentration. Device structure was ITO/DNTPD/NPB/TCTA/BSFM:Ir(pq)<sub>2</sub>acac/TSPO1/LiF/Al.

of Ir(ppy)<sub>3</sub> were 3%, 5% and 10%. The hole transport material was mCP and the electron transport material was TSPO1. There was no energy barrier for charge injection for the charge transport materials in the TPBI device. Quantum efficiency–luminance curves of the TPBI:Ir(ppy)<sub>3</sub> green PHOLEDs are shown in Fig. 11 according to the Ir(ppy)<sub>3</sub> doping concentration. The device performances were optimized at a doping concentration of 3% and the quantum efficiency was a little lowered at high doping concentration. Similar to other PHOLEDs fabricated in this work, an optimized doping concentration of 3%, little efficiency roll-off and little reduction of the quantum efficiency at high doping concentration were observed in the TPBI:Ir(ppy)<sub>3</sub> PHOLEDs, as there was no energy barrier for charge injection.

Red PHOLEDs with an Ir(pq)<sub>2</sub>acac doped BSFM emitting layer were also fabricated to prove that device performances can be optimized irrespective of the dopant material. Quantum efficiency–luminance curves of the BSFM:Ir(pq)<sub>2</sub>acac PHOLEDs are shown in Fig. 12. The hole transport material was TCTA and the electron transport material was TSPO1. The energy barrier for hole injection was 0.2 eV and that for electron injection was 0 eV. The



quantum efficiency was also optimized at 3%, as it was for green-emitting BSFM:Ir(ppy)<sub>3</sub> PHOLEDs. Although the dopant material was changed, the optimum doping concentration was not affected. As charge injection and transport by the host material and light emission by energy transfer are dominant, the dopant material had little effect on the optimum doping concentration.

Therefore, it can be concluded that the quantum efficiency of PHOLEDs can be optimized at a low doping concentration below 5% by engineering the hole and electron transport materials. This work discovered and proved that the optimum doping concentration of PHOLEDs is below 5%, as observed for fluorescent organic light emitting diodes.

#### 4. Conclusions

In conclusion, engineering of the energy levels of the charge transport materials revealed that the optimum doping concentration of PHOLEDs is below 5% irrespective of the host material. The trapping of charge carriers by the dopant was responsible for the high doping concentration of PHOLEDs; hence suppression of charge trapping by management of the charge transport materials enabled the quantum efficiency to be optimized at a low doping concentration of 3%. This work may enable the fabrication of PHOLEDs with universally low optimum doping concentrations and could be useful for the future development of high efficiency PHOLEDs. This concept can also reduce the production cost of OLED panels by reducing the amount of dopant used.

#### References

- [1] M.A. Baldo, D.F. Brien, Y. You, A. Shoustikov, S. Sibley, M.E. Thompson, S.R. Forrest, Highly efficient phosphorescent emission from organic electroluminescent devices, *Nature* 395 (1998) 151.
- [2] H. Sasabe, T. Chiba, S.-J. Su, Y.J. Pu, K.I. Nakayama, J. Kido, 2-Phenylpyrimidine skeleton-based electron-transport materials for extremely efficient green organic light-emitting devices, *Chem. Commun.* 44 (2008) 5821.
- [3] S.-J. Su, E. Gonmori, H. Sasabe, J. Kido, Highly Efficient Organic Blue and White-Light-Emitting Devices Having a Carrier- and Exciton-Confining Structure for Reduced Efficiency Roll-Off, *Adv. Mater.* 20 (2008) 4189.
- [4] N. Chopra, J. Lee, Y. Zheng, S.-H. Eom, J. Xue, F. So, High efficiency blue phosphorescent organic light-emitting device, *Appl. Phys. Lett.* 93 (2008) 143307.
- [5] S.O. Jeon, S.E. Jang, H.S. Son, J.Y. Lee, External Quantum Efficiency Above 20% in Deep Blue Phosphorescent Organic Light-Emitting Diodes, *Adv. Mater.* 23 (2011) 1436.
- [6] S. Yeh, M. Wu, C. Chen, Y. Song, Y. Chi, M. Ho, S. Hsu, C.H. Chen, New Dopant and Host Materials for Blue-Light-Emitting Phosphorescent Organic Electroluminescent Devices, *Adv. Mater.* 17 (2005) 285.
- [7] D.M. Kang, J.-W. Kang, J.W. Park, S.O. Jung, S.-H. Lee, H.-D. Park, Y.-H. Kim, S.C. Shin, J.-J. Kim, S.-K. Kim, Iridium Complexes with Cyclometalated 2-Cycloalkenyl-Pyridine Ligands as Highly Efficient Emitters for Organic Light-Emitting Diodes, *Adv. Mater.* 20 (2008) 2003.
- [8] M.-H. Tsai, H.-W. Lin, H.-C. Su, T.-H. Ke, C.-C. Wu, F.-C. Fang, Y.-L. Liao, K.-T. Wong, C.-I. Wu, Highly Efficient Organic Blue Electrophosphorescent Devices Based on 3,6-Bis(triphenylsilyl)carbazole as the Host Material, *Adv. Mater.* 18 (2007) 1216.
- [9] Y. Tao, Q. Wang, C. Yang, C. Zhong, J. Qin, D. Ma, Multifunctional Triphenylamine/Oxadiazole Hybrid as Host and Exciton-Blocking Material: High Efficiency Green Phosphorescent OLEDs Using Easily Available and Common Materials, *Adv. Funct. Mater.* 20 (2010) 2923.
- [10] W.S. Jeon, T.J. Park, S.Y. Kim, R. Pode, J. Jang, J.H. Kwon, Ideal host and guest system in phosphorescent OLEDs, *Org. Electron.* 10 (2009) 240.
- [11] S.O. Jeon, K.S. Yook, C.W. Joo, J.Y. Lee, Theoretical maximum quantum efficiency in red phosphorescent organic light-emitting diodes at a low doping concentration using a spirobenzofluorene type triplet host material, *Org. Electron.* 11 (2010) 881.
- [12] K. Okumoto, H. Kanno, Y. Hamaa, H. Takahashi, K. Shibata, Green fluorescent organic light-emitting device with external quantum efficiency of nearly 10%, *Appl. Phys. Lett.* 89 (2006) 063504.
- [13] M.-T. Lee, C.-H. Liao, C.-H. Tsai, C.H. Chen, Highly efficient, deep-blue doped organic light-emitting devices, *Adv. Mater.* 17 (2005) 2493.
- [14] J. Yang, J. Shen, Doping effects in organic electroluminescent devices, *J. Appl. Phys.* 84 (1998) 2105.
- [15] L.I. Liu, C.P. Palsule, S. Gangopadhyay, W.L.J. Borst, Intermolecular energy transfer in binary systems of dye polymers, *J. Appl. Phys.* 88 (2000) 4860.
- [16] R.J. Holmes, B.W. D'Andrade, S.R. Forrest, X. Ren, J. Li, M.E. Thompson, Efficient, deep-blue organic electrophosphorescence by guest charge trapping, *Appl. Phys. Lett.* 83 (2003) 3818.
- [17] J. Lee, J.-I. Lee, K.-I. Song, S.J. Lee, H.Y. Chu, Effects of interlayers on phosphorescent blue organic light-emitting diodes, *Appl. Phys. Lett.* 92 (2008) 203305.
- [18] Y. Zheng, S.-H. Eom, N. Chopra, J. Lee, F. So, J. Xue, Efficient deep-blue phosphorescent organic light-emitting device with improved electron and exciton confinement, *Appl. Phys. Lett.* 92 (2008) 223301.
- [19] R.J. Holmes, S.R. Forrest, Y.-J. Tung, R.C. Kwong, J.J. Brown, S. Garon, M.E. Thompson, Blue organic electrophosphorescence using exothermic host-guest energy transfer, *Appl. Phys. Lett.* 82 (2003) 2422.
- [20] K.S. Yook, S.O. Jeon, C.W. Joo, J.Y. Lee, High efficiency deep blue phosphorescent organic light-emitting diodes, *Org. Electron.* 10 (2009) 170.
- [21] J.-H. Lee, C.-L. Huang, C.-H. Hsiao, M.-K. Leung, C.-C. Yang, C.-C. Chao, Blue phosphorescent organic light-emitting device with double emitting layer, *Appl. Phys. Lett.* 94 (2009) 223301.